Etude de l'initiation et de la propagation de l'auto-inflammation dans un milieu présentant des inhomogénéités de température

Guillaume Lodier[a,b], Pascale Domingo[a], Luc Vervisch[a]

a. *CORIA-CNRS et INSA de Rouen, Technopole du Madrillet, 76801 Saint-Etienne-du-Rouvray, France*
b. *RENAULT - Technocentre 1, avenue du Golf 78288 Guyancourt cedex, France*

Résumé :

Cette étude se focalise sur le phénomène d'auto-allumage caractérisé par une initiation spontanée de la combustion suite à une forte compression. Des simulations numériques sont réalisées dans une configuration de Machine à Compression Rapide (MCR). Dans un premier temps, les résultats de simulations aux grandes échelles d'un écoulement inerte sont comparés à des mesures expérimentales. Ensuite, la simulation directe bidimensionnelle d'un écoulement réactif dans cette MCR est utilisée pour analyser les mécanismes contrôlant la formation des noyaux précurseurs de l'allumage. Trois scénari d'interaction entre les champs thermochimique et aérodynamique sont ainsi mis en évidence.

Abstract :

The processes involved in autoignition phenomenon, which is characterised by a spontaneous initiation of the combustion as a result of a strong compression, are investigated in the present study. Numerical simulation of a flow generated by a Rapid Compression Machine (RCM) are performed. First, results of a Large Eddy Simulation of an inert flow are compared with those of an experiment. Then, the two-dimensional Direct Numerical simulation of a reactive flow is used to look into the mechanisms controlling the selection of the precursor nuclei of autoignition. Three interactions between aerodynamic- and thermochemical-field are highlighted.

Mots clefs : Autoignition ; Simulation Numérique Directe ; Machine à Compression Rapide

1 Introduction

Carmakers have to meet increasingly stringent emission norms. Thus, technological breakthrough must be imagined and for this purpose, it is necessary to have a deep insight into the highly unsteady behavior of turbulent flames in an engine, specifically the auto-ignition phase, which depends on strongly non-linear phenomena, must be fully under control. Some important issues still need to be examined concerning the genesis of ignition kernels after a rapid compression, often referred as 'hot spots' as temperature plays a first order role in the initiation of combustion, as well as their interactions once one, or some of them, begin to develop. In the following, it is shown that at least three mechanisms enter the coupling between the aerodynamic fields and thermochemistry in the formation of reactive kernels. First, the pressure decrease at the center of the turbulent structures leads to lower reactivity of the medium. Second, this effect is counterbalanced by the fact that the fluid trapped in the core of these vortices is thermally insulated from the rest of the flow, thus avoiding thermal leakage if temperature at the vortex core allows for primary ignition. Third, local compressibility effects, which intensity is measured by the divergence of the velocity field, on the other hand locally increase the reactivity.

2 Three-dimensional Large Eddy Simulation of the RCM

The fully compressible finite volume SiTCom (Simulating Turbulent Combustion) LES & DNS code is used [6]. The flow inside the combustion chamber of the RCM experimentally studied in [3] is first simulated when a non-reactive mixture is admitted. The combustion chamber is a cylinder of diameter 4 cm and of length 4.4 cm represented in SiTCom with immersed boundaries. The LES filter is $\Delta = 0.24$ mm with a 4 million mesh. The effect of the piston in the compression is mimicked using a mean velocity inlet profile $< U(t, r, \theta) >$, which is assumed axisymmetric and self-similar in time :

$$< U(t, r, \theta) >= U_n(t)\, p(r) \tag{1}$$

where $U_n(t)$ is the average normal velocity of the flow at the inlet and $p(r)$ is the spatial shape of the inlet profile. On the top of this profile, turbulence is added [4] according to the grid properties located at the inlet of the cylinder. $U_n(t)$ can be expressed as a function of the speed and the position of the piston reported from the experiment :

$$U_n(t) = \frac{D_{cc}^2 L_{cc}}{D_p^2 L^* + D_p^2 (x_p(t) - x^*) + D_{cc}^2 L_{cc}} \left(\frac{D_p}{D_{cc}}\right)^2 \dot{x}_p(t) \tag{2}$$

where D_{cc} and L_{cc} are the diameter and the height of the combustion chamber, L^* is an estimation of the dead-volume characteristic length, D_p is the piston diameter, x_p the piston position, x^* refers to the dead-volume and $\dot{x}_p$ is the piston-speed. With this expression, the time evolution of pressure perfectly reproduces the experiment (Fig. 1).

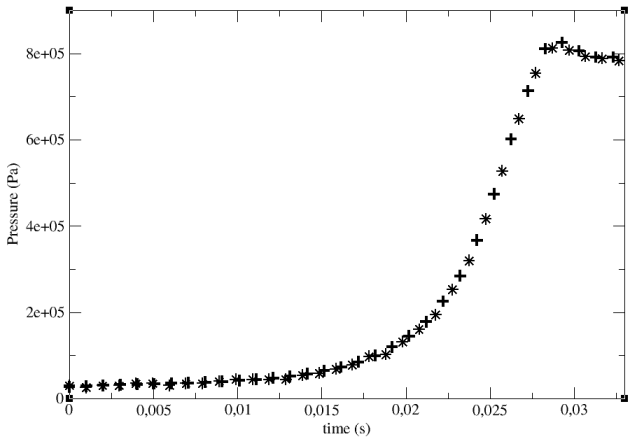

FIGURE 1 – Time histories of pressure. Stars : experiment. Plus : LES, pressure averaged over the whole domain.

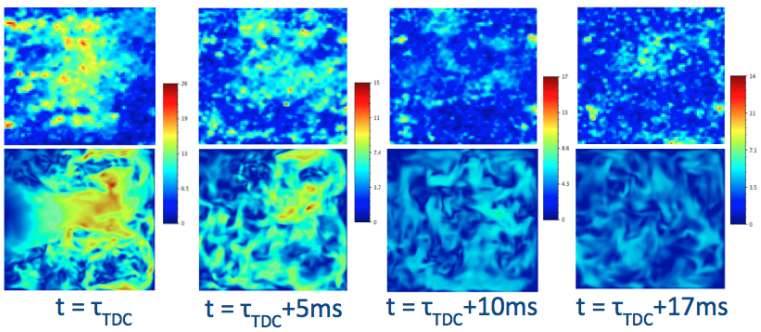

FIGURE 2 – Fields of velocity magnitude at representative instants after top dead center. Top : PIV. Bottom : LES.

Regarding the aerodynamic details, various $p(r)$ distributions have been tested to compare LES against Particle Image Velocimetry measurements. For some of the $p(r)$ that have been tested, a

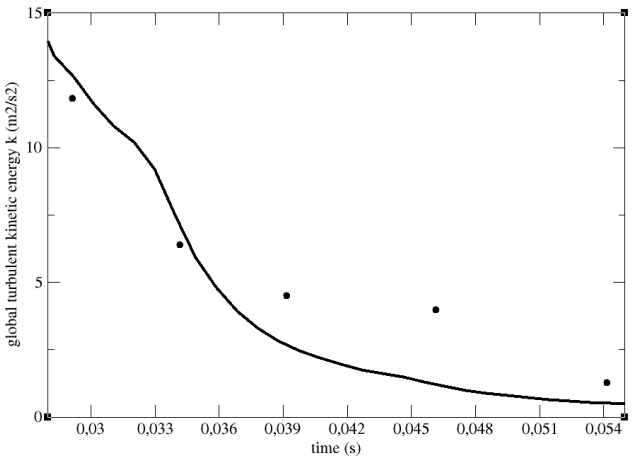

FIGURE 3 – Turbulent kinetic energy *vs* time. Symbols : PIV. Line : LES.

Kelvin-Helmholtz instability develops, which is not found in the experiment. To prevent it, the Rayleigh criterion has to be satisfied and $p(r)$ may not contain any inflection point. Second, the levels of the velocity magnitude should be the reproduced (Fig. 2). Last, the turbulent kinetic energy magnitude averaged over the median plane of the combustion chamber should also be representative of the one obtained by PIV (see Fig. 3). This parametrization leads to $p(r)$ expressed as an hyperbolic tangent of the radius.

3 Two-dimensional Direct Numerical Simulation of the reactive flow

To reduce the numerical effort allowing for DNS, the geometry of the combustion chamber has been downsized four times in each direction, the mesh contains 530×514 cells of about 20 micron-meter. The wall temperature is computed with a convection coefficient fixed at 40 $W.m^{-1}.K^{-1}$. Single-step chemistry is used, two cases are considered keeping fixed the pre-exponential factor, but varying the activation temperature so that ignition occurs at $\tau_1 = 0.0283\ s$ in case 1 and $\tau_2 = 0.0329\ s$ in case 2, when the top dead center is reached at $\tau_{TDC} = 0.0292\ s$. Admission turbulence intensity is higher in case 1 (30%) than in case 2 (10%).

To analyze results, the temperature balance equation may be cast in :

$$\frac{DT}{Dt} = \underbrace{\frac{\gamma}{\rho C_p}\dot{\omega}_T}_{\text{Term (1)}} + \overbrace{(1-\gamma)T\nabla\cdot\mathbf{u}}^{\text{Term (2)}} + \underbrace{\frac{\gamma}{\rho}\nabla\cdot(\rho D_{th}\nabla T)}_{\text{Term (3)}} \tag{3}$$

The first term is representative of chemistry effects, the second captures compressibility, the last is molecular diffusion. For chemistry to be initiated at a given point, a local temperature rise (hot spot) is needed. From Eq. 3, it is seen that compressibility (Term (2)) and diffusion of heat (Term (3)) compete. In a spatially weakly-varying temperature field, it is mainly compressibility that will first controls ignition. Figure 4 is extracted from the computation of case 1, in the zone where combustion starts. Here the fluid is pulled forward by two counterrotating vortices because of viscous shear effects. While considering this process as being quasi-steady, streamlines merge with the trajectories of the fluid particles. In the same way as an incompressible flow, the narrowing of the cross-sectional area and the resulting streamlines constriction between the vortices generate the increase of the velocity magnitude (see colors on the streamlines, where blue stands for 0 m/s and red, for the 20 m/s). Differences between incompressible and compressible cases arise because of the confinement that prevents the volumetric flow rate from being conserved : the compressible bulk velocity is less than the incompressible one and $\nabla\cdot\mathbf{u}$ is locally negative, meaning that Term (2) in Eq. 3 is positive and

reaches higher values (see the grey levels on Fig. 4). Consequently, this mechanism may participate to the formation of primary hot spots.

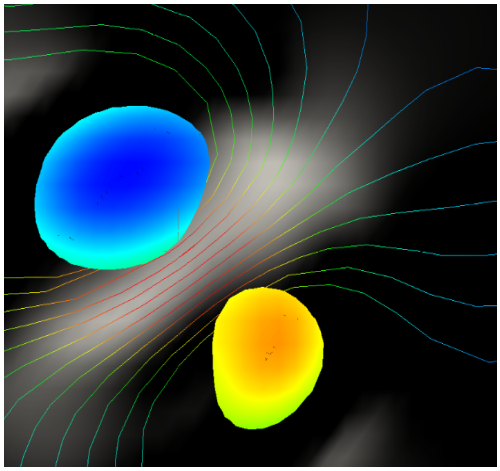

FIGURE 4 – The value of the velocity magnitude, here only given on the streamlines, is increased between the counterrotative vortices.

Aside from the strained zone, vortices core are found, which contribute to ignition according to two counterbalancing mechanisms. Figure 5 is extracted from the computation of case 1 (on the top) and 2 (at the bottom). Colors in the left picture stand for the values of the Q-criterion making possible to locate the turbulent structures, while grey levels represent the values of the temperature dissipation rate $\chi_T = \rho D_{th} |\nabla T|^2$ that is here used to track the temperature inhomogeneities. In both cases, χ_T wraps around the main rotating structures without penetrating them. Simultaneously, at the center of the vortices, the pressure decreases according to the following equality :

$$Q = \frac{1}{2\rho} \Delta P \tag{4}$$

The pictures at the center of Fig. 5 is an obvious illustration of this relationship between the velocity (isocontour of the Q-criterion) and the pressure field (in grey levels).

In case 1 (Fig. 5-top), this pressure drop can be readily associated with a decrease of the chemical source term magnitude. Indeed, the central vortex that stands for the lowest pressure in the domain corresponds to a local minimum of heat release, hence combustion does not start within the vortex but in the local compression zone bordering the high vorticity region. The opposite behavior is observed in case 2 (Fig. 5-bottom), where it is rather the small temperature dissipation rate (therefore molecular diffusion) that favor ignition within the vortex.

The difference in local flow properties promoting these various ignition behaviors relate to variability of global quantities. First, it should be kept in mind that the turbulent intensity is higher in case 1 than in case 2. Second, autoignition in case 1 occurs earlier than in case 2, where turbulence has already decayed. Implications of these two remarks regarding the global turbulent kinetic energy can be observed in Fig. 6. This average behavior of the turbulent kinetic energy may be related to the local vortices properties, where qualitative differences between case 1 and case 2 are quantified by comparing the values of the Q-criterion and the pressure drop inside the central turbulent structures in each case. In case 1, the Q-criterion is of the order of $10^{10}\ s^{-1}$ and the pressure drop, of the order of $10^4\ Pa$. In case 2, both of them are dramatically reduced, that is to say, respectively to $10^8\ s^{-1}$ and $10^3\ Pa$: the mechanism described by equation 4 is of weak importance compared to the thermal insulation (lack of molecular diffusion within the core of the vortex) phenomenon which dominates here in an obvious manner, then ignition occurs at the core of the vortex, while it is located in a local compression zone in case 1.

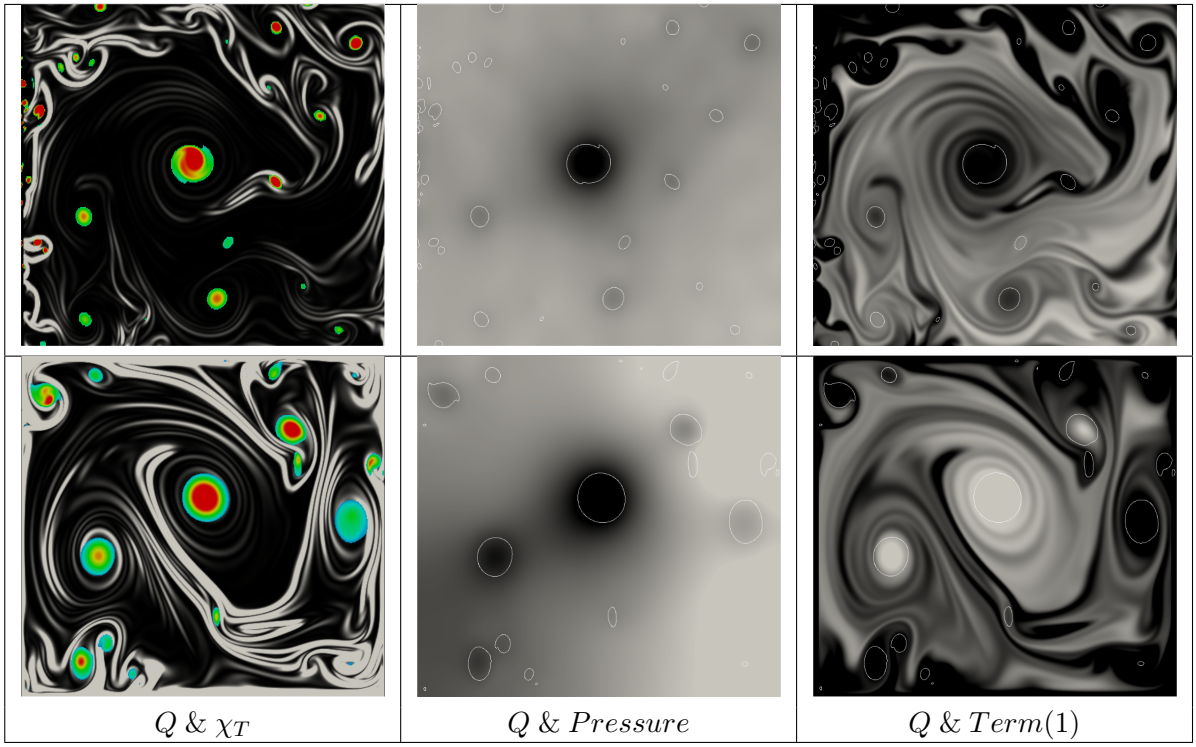

FIGURE 5 – Top : case 1. Bottom : case 2. Coupling mechanisms between the aerodynamic and the thermo-chemical fields. From left to right : Q-criterion (in color) & temperature scalar disspation rate (in grey levels) ; isocontour of Q-criterion (white line) & pressure (in grey levels) ; isocontour of Q-criterion (white line) & value of term (1) (in grey levels)

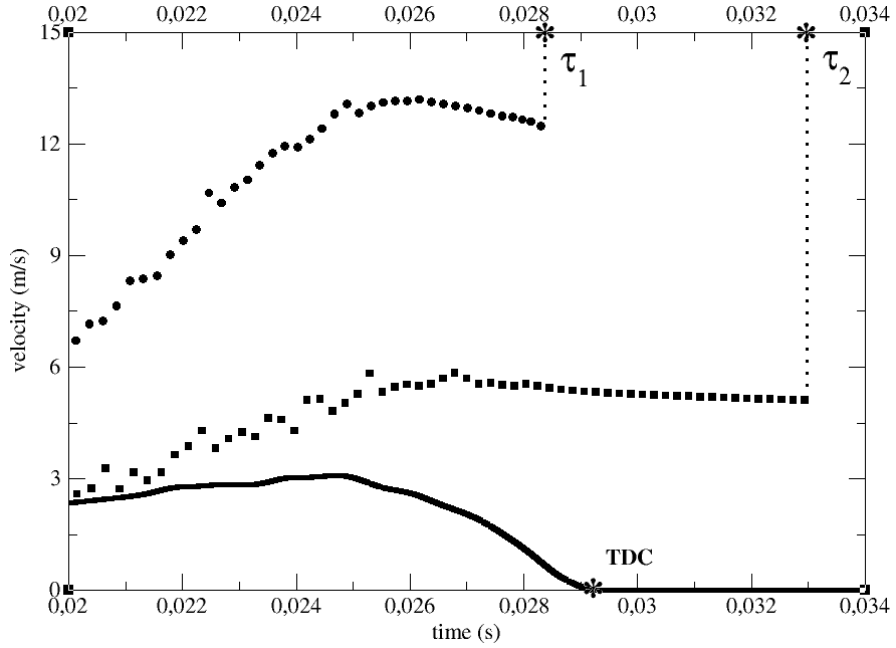

FIGURE 6 – Bold line : velocity of the piston. Symbols : spatial average velocity fluctuation in the combustion chamber. Case 1 : circles. Case 2 : squares.

4 Conclusion

Three-dimensional Large Eddy Simulation of a rapid compression machine was performed to calibrate DNS of the same flow problem, after downsizing its geometry. LES is used to parameterize an inlet velocity profile, making it possible to obtain realistic time history of the quantities related to thermodynamic and aerodynamic fields without having to simulate the full compression machine, but only the combustion chamber. With these conditions, a two-dimensional DNS of a reactive flow in the downsized combustion chamber has been conducted for two activation temperatures. Three mechanisms coupling the aerodynamic to thermochemistry and promoting different scenarios for the formation of very primary hot spots have been underlined :

1. local compression phenomena, tracked by the divergence of the velocity, increases the local reactedness of the mixture ;
2. pressure drop at the vortex core diminishes the temperature and the chemical source as well ;
3. the fluid trapped in the vortex core may benefit from 'thermal insulation' from the rest of the flow ; which can counterbalance the previous mechanism.

This study will be continued with three-dimensional DNS including multi-step chemistry in order to account for vortex stretching in the third direction and for the impact of radical species dissociation.

Références

[1] Balaras, E. 2004 Modeling complex boundaries using an external force field on fixed Cartesian grids in large eddy simulations. *Computers and Fluids* **33 (3)**, 375-404

[2] Fadlun E. A. , Verzicco R. , Orlandi P. and Mohd-Yusof J. 2000 Combined Immersed- Boundary Finite-Difference Methods for Three-Dimensional Complex Flow Simulations. *J. Comput. Phys.* **161**, 35-60

[3] Guibert P., Keromnes A. and Legros G. 2009 An Experimental Investigation of the Turbulence Effect on the Combustion Propagation in a Rapid Compression Machine *Flow Turbulence Combustion* **84**, 79-95

[4] Klein M., Sadiki A. and Janicka J. 2003 A digital filter based generation of inflow data for spatially developing direct numerical or large eddy simulations. *Journal of Computational Physics* **186**, 652–665

[5] Iaccarino G. and Verzicco R. 2003 Immersed boundary technique for turbulent flow simulations. *Appl. Mech. Rev.* **56 (3)**, 331-347

[6] Lodato G., Domingo P. and Vervisch L. 2008 Three-Dimensional boundary conditions for direct and large eddy simulation of compressible viscous flows. *J. Comput. Phys.* **227 (10)**, 5105-5143

[7] Poinsot T. and Veynante D. 2005 Theoritical and Numerical Combustion. *R. T. Edwards*

[8] Veynante D. and Vervisch L. 2002 Turbulent Combustion Modeling. *Progress in Energy and Combustion Science* **28 (3)**, 193-266